Inorg. Chem. **2005**, *44*, 1660–1671

The Highest Bond Order Between Heavier Main-Group Elements in an Isolated Compound? Energetics and Vibrational Spectroscopy of $S_2I_4(MF_6)_2$ (M = As, Sb)

Scott Brownridge,[†] T. Stanley Cameron,[‡] Hongbin Du,[†] Carsten Knapp,[†] Ralf Köppe,[§] Jack Passmore,*[,†,⊥] J. Mikko Rautiainen,[∥] and Hansgeorg Schnöckel[§]

Department of Chemistry, University of New Brunswick, Fredericton, New Brunswick E3B 6E2, Canada, Department of Chemistry, Dalhousie University, Halifax, Nova Scotia B3H 4J3, Canada, Institut für Anorganische Chemie, Universität Karlsruhe, 76131 Karlsruhe, Germany, and Department of Chemistry, University of Jyväskylä, 40500 Jyväskylä, Finland

Received July 20, 2004

The vibrational spectra of $S_2I_4(MF_6)_2$(s) (M = As, Sb), a normal coordinate analysis of $S_2I_4^{2+}$, and a redetermination of the X-ray structure of $S_2I_4(AsF_6)_2$ at low temperature show that the S–S bond in $S_2I_4^{2+}$ has an experimentally based bond order of 2.2–2.4, not distinguishably different from bond orders, based on calculations, of the Si–Si bonds in the proposed triply bonded disilyne of the isolated $[(Me_3Si)_2CH]_2(^iPr)SiSiSi(^iPr)[CH(SiMe_3)_2]_2$ and the hypothetical *trans*-RSiSiR (R = H, Me, Ph). Therefore, both $S_2I_4^{2+}$ and $[(Me_3Si)_2CH]_2(^iPr)SiSiSi(^iPr)[CH(SiMe_3)_2]_2$ have the highest bond orders between heavier main-group elements in an isolated compound, given a lack of the general acceptance of a bond order > 2 for the Ga–Ga bond in $Na_2[\{Ga(C_6H_3Trip_2\text{-}2,6)\}_2]$ (Trip = $C_6H_2Pr^i_3$-2,4,6) and the fact that the reported bond orders for the heavier group 14 alkyne analogues of formula REER [E = Ge, Sn, or Pb; R = bulky organic group] are ca. 2 or less. The redetermination of the X-ray structure gave a higher accuracy for the short S–S [1.842(4) Å, Pauling bond order (BO) = 2.4] and I–I [2.6026(9) Å, BO = 1.3] bonds and allowed the correct modeling of the AsF_6^- anions, the determination of the cation–anion contacts, and thus an empirical estimate of the positive charge on the sulfur and iodine atoms. FT-Raman and IR spectra of both salts, obtained for the first time, were assigned with the aid of density functional theory calculations and gave a stretching frequency of 734 cm^{-1} for the S–S bond and 227 cm^{-1} for the I–I bond, implying bond orders of 2.2 and 1.3, respectively. A normal-coordinate analysis showed that no mixing occurs and yielded force constants for the S–S (5.08 mdyn/Å) and I–I bonds (1.95 mdyn/Å), with corresponding bond orders of 2.2 for the S–S bond and 1.3 for the I–I bond, showing that $S_2I_4^{2+}$ maximizes π bond formation. The stability of $S_2I_4^{2+}$ in the gas phase, in SO_2 and HSO_3F solutions, and in the solid state as its AsF_6^- salts was established by calculations using different methods and basis sets, estimating lattice enthalpies, and calculating solvation energies. Dissociation reactions of $S_2I_4^{2+}$ into various small monocations in the gas phase are favored [e.g., $S_2I_4^{2+}(g) \rightarrow 2SI_2^+(g)$, $\Delta H = -200$ kJ/mol], as are reactions with I_2 [$S_2I_4^{2+}(g) + I_2(g) \rightarrow 2SI_3^+(g)$, $\Delta H = -285$ kJ/mol). However, the corresponding reactions in the solid state are endothermic [$S_2I_4(AsF_6)_2(s) \rightarrow 2SI_2(AsF_6)(s)$, $\Delta H = +224$ kJ/mol; $S_2I_4(AsF_6)_2 + I_2(s) \rightarrow 2SI_3(AsF_6)(s)$, $\Delta H = +287$ kJ/mol). Thus, $S_2I_4^{2+}$ and its multiple bonds are *lattice stabilized* in the solid state. Computational and FT-Raman results for solution behavior are less clear cut; however, $S_2I_4^{2+}$ was observed by FT-Raman spectroscopy in a solution of HSO_3F/AsF_5, consistent with the calculated small, positive free energies of dissociation in HSO_3F.

1. Introduction

For many years, there has been considerable interest in the preparation of stable compounds containing homonuclear heavy (n ≥ 3) main-group multiple-bonded atoms.[1−7] Recent investigations of homonuclear multiple bonds between the elements of groups 13 and 14 containing bulky substituents are the subject of continuing controversy and current research. The proposed Ga−Ga triple bond in $Na_2[\{Ga(C_6H_3\text{-}Trip_2\text{-}2,6)\}_2]$ (Trip = $C_6H_2Pr^i_3$-2,4,6)[2] has not been generally accepted.[1d,e,3c] The geometry of H−C≡C−H, containing a carbon−carbon triple bond, is linear; however, the geometries of $[RGaGaR]^{2-}$ and REER (E = Si, Ge, Sn, or Pb; R = bulky organic group) are bent. Nevertheless, some claim

* E-mail: passmore@unb.ca. Fax: 1-506-453-4981. Tel: 1-506-453-4821.
[†] Univeristy of New Brunswick.
[‡] Dalhousie University.
[§] Universität Karlsruhe.
[∥] Univeristy of Jyväskylä.
[⊥] Part of this work was presented at the 9th International Conference on Inorganic Ring Systems, Saarbrücken, Germany, and at the 16th International Symposium—Fluorine Chemistry, Durham, U.K., in July 2000.

10.1021/ic049035g CCC: $30.25
Published on Web 02/18/2005

there is a triple bond in these compounds,[2] which some view as a "slipped" triple bond.[3a] Others have proposed, from a consideration of relative bond distances and the nonlinearity along the multiple bond, that the structures can be described by two valence bond structures, one with a triple bond and another with a lone pair on each of the atoms, resulting in a bond order of significantly less than 3.[1e] This model is supported by a quantitative electron localization function (ELF) study;[3b] however, a qualitative treatment using an ELF analysis takes a different view.[3a] In 2002, Power and coworkers obtained the X-ray structure of RGeGeR (R = C_6H_3-2,6-$Dipp_2$; Dipp = C_6H_3-2,6-$^iPr_2$).[1j,4] It was also bent, with a Ge−Ge bond distance corresponding to a bond order of about 2. Currently, evidence for a disilyne in solution has been published,[5a,d] and after this paper was accepted for publication, a crystal structure of the bent disilyne [$(Me_3Si)_2CH]_2(^iPr)SiSiSiSi(^iPr)[CH(SiMe_3)_2]_2$ was obtained with a calculated [B3LYP/6-31G(d)] Wiberg bond index of 2.618.[5e,f] Topological bond orders for *trans*-RSiSiR were calculated[3b] (B3LYP/cc-pVDZ) as 2.0 (R = H) and 1.9 (R = Me) and, by the method of Mayer[3c] [B3LYP/6-311G(d,p) level], as 2.37 (R = H), 2.30 (R = Me), and 2.20 (R = Ph).

Whereas bulky groups have been used to stabilize multiply bonded species of the heavier elements of groups 13−15, numerous examples of such compounds containing the elements of groups 16 and 17 have been known for decades.[6−9] This is especially true for compounds containing sulfur, for example, thiothionyl fluoride S═SF_2, which has an S−S bond distance less than that of S_2(g) and a bond order slightly greater than 2 (Table 1). Some time ago, we reported the crystal structures of $S_2I_4(MF_6)_2$ (M = As or Sb),[10] which have the shortest S−S bond lengths reported for an isolated compound [1.854(6) and 1.818(10) Å], corresponding to Pauling bond orders of 2.4 and 2.7, respectively. $S_2I_4^{2+}$ maximizes π bonding, even though it is not sterically prevented from isomerizing to the σ bonded alternative structure that is analogous to that of P_2I_4.[52]

Table 1. Selected Examples of Species Containing S−S or I−I Bond Orders (BO) ≥ 1

compound	d_{SS} [Å]	ν_{SS} [cm^{-1}]	f_{SS} (exp.) [mdyn/Å]	BO by definition
S_8(s)	2.06[a,53]	475[b]	2.37[53]	
H−S−S−H(g)	2.055(2)[53]	516[40]	2.58[53]	1
S_4^{2+}(s)	2.011(3)[a,46]	584[53]		1.25
S_2^-(g)	2.00[40]	600[40]	3.35[c]	1.5
S_7I^+(s)	1.906(5)[d,54]	618[55]		
F−S−S−F(g)	1.890(2)[56]	615[40]	3.47[38]	
S═S═O(g)	1.882[53]	680[40]	4.7[53]	
S_2(g)	1.892[53]	700[40]	4.89[40]	2
S═SF_2(g)	1.856(2)[56]	761[49]	5×10^{38}	
$S_2I_4(AsF_6)_2$(s)	1.842(4)[e]	734[e,b]	5.08[e]	
$S_2I_4(SbF_6)_2$(s)	1.818(10)[10]	732[e,b]		
S_2^+(g)	1.82[40]	790[40]	5.88[40]	2.5

compound	d_{II} [Å]	ν_{II} [cm^{-1}]	f_{II} (exp.) [mdyn/Å]	BO by definition
I_2^-(s)		115[57]	0.49[57]	0.5
I_2(s)	2.715(6)[58]	180[f,34]		
I_2(g)	2.66[40]	214[40]	1.72[40]	1
$S_2I_4(AsF_6)_2$(s)	2.6026(9)[e]	228[e,b]	1.95[e]	
$S_2I_4(SbF_6)_2$(s)	2.571(2)[10]	227[e,b]		
I_2^+(s)	2.557(4)[59]	238[59]	2.15[40]	1.5

[a] Corrected for the libration motions. [b] FT-Raman spectra. [c] Calculated from the inharmonic stretching frequency. [d] The shortest S−S bond in S_7I^+. [e] This work. [f] Matrix-isolated I_2 monomers give a Raman frequency of 212 cm^{-1}.[60]

To further clarify the nature of the structure and bonding in $S_2I_4^{2+}$, infrared and FT-Raman spectra for $S_2I_4(MF_6)_2$ are reported for the first time in this paper, assignments made based on density functional thory (DFT) calculations, and a normal-coordinate analysis of the vibrational spectra carried out. Previous attempts to obtain FT-Raman spectra were unsuccessful, and IR spectra only gave peaks due to the anions.[10] This paper also reports solution FT-Raman spectra of $S_2I_4(AsF_6)_2$ in both SO_2 and HSO_3F to investigate the nature of the species in solution. It was reported earlier that the solubility of $S_2I_4(AsF_6)_2$ in SO_2 increased dramatically

(1) (a) Cowley, A. H. *Polyhedron* **1984**, *3*, 389−432. (b) Cowley, A. H. *Acc. Chem. Res.* **1984**, *17*, 386−392. (c) *Multiply Bonded Main Group Metals and Metalloids*; West, R., Stone, F. G. A., Eds.; Academic Press: San Diego, CA, 1996. (d) Power, P. P. *J. Chem. Soc., Dalton Trans.* **1998**, 2939−2951. (e) Power, P. P. *Chem. Rev.* **1999**, *99*, 3463−3503. (f) Robinson, G. H. *Adv. Organomet. Chem.* **2001**, *47*, 283−294. (g) West, R. *Polyhedron* **2002**, *21*, 467−472. (h) Weidenbruch, M. *Organometallics* **2003**, *22*, 4348−4360. (i) Weidenbruch, M. *Angew. Chem.* **2003**, *115*, 2322−2324; *Angew. Chem., Int. Ed. Engl.* **2003**, *42*, 2222−2224. (j) Power, P. P. *Chem. Commun.* **2003**, 2091−2101. (k) Iwamoto, T.; Kira, M. *J. Synth. Org. Chem., Jpn.* **2004**, *62*, 94−106.

(2) (a) Xie, Y.; Schaefer, H. F., III; Robinson, G. H. *Chem Phys. Lett.* **2000**, *317*, 174−180. (b) Xie, Y.; Grev, R. S.; Gu, J.; Schaefer, H. F., III; Schleyer, P. v. R.; Su, J.; Li, X.-W.; Robinson, G. H. *J. Am. Chem. Soc.* **1998**, *120*, 3773−3780. (c) Robinson, G. H. *Acc. Chem. Res.* **1999**, *32*, 773−782. (d) Weidenbruch, M. *Angew. Chem., Int. Ed. Engl.* **2005.** *44*, 514−516.

(3) (a) Grützmacher, H.; Fässler, T. F. *Chem.−Eur. J.* **2000**, *6*, 2317−2325. (b) Malcom, N. O. J.; Gillespie, R. J.; Popelier, P. L. A. *J. Chem Soc., Dalton Trans.* **2002**, 3333−3341. (c) Bridgeman, A. J.; Ireland, L. R. *Polyhedron* **2001**, *20*, 2841−2851.

(4) Stender, M.; Phillips, A. D.; Wright, R. J.; Power, P. P. *Angew. Chem.* **2002**, *114*, 1863−1865; *Angew. Chem., Int. Ed.* **2002**, *41*, 1785−1787.

(5) (a) Wiberg, N.; Niedermayer, W.; Fischer, G.; Nöth, H.; Suter, M. *Eur. J. Inorg. Chem.* **2002**, 1066−1070. (b) Takagi, N.; Nagase, S. *Chem. Lett.* **2001**, 966−967. (c) Takagi, N.; Nagase, S. *Eur. J. Inorg. Chem.* **2002**, 2775−2778. (d) Wiberg, N.; Vasisht, S. K.; Fischer, G.; Mayer P. *Z. Anorg. Allg. Chem.* **2004**, *630*, 1823−1828. (e) Sekiguchi, A.; Kinjo, R.; Ichinohe, M. *Science* **2004**, *305*, 1755−1757. (f) West, R. *Science* **2004**, *305*, 1724−1725.

(6) Examples containing heavier groups 16 and 17 elements are M_4^{2+} (M = S, Se, Te), X_2^+ (X = Br, I),[7] $M_3X_3^+$ (M = S, Se; X = Cl, Br),[8] and some 1,2-dications related to $S_2I_4^{2+}$.[11]

(7) (a) Gillespie, R. J.; Passmore, J. *Adv. Inorg. Chem. Radiochem.* **1975**, *17*, 49−87. (b) Gillespie, R. J.; Passmore, J. *International Review of Science, Inorganic Chemistry Series Two*; Butterworth and University Press: London, 1975; Vol. 3, pp 121−136. (c) Passmore, J. *Homoatomic Rings, Chains and Macromolecules of Main Group Elements*; Elsevier Scientific: New York, 1977; pp 539−550. (d) Burford, N.; Passmore, J.; Sanders, J. C. P. In *From Atoms to Polymers, Isoelectronic Analogies*; Liebmann, J. F., Greenburg, A., Eds.; VCH: New York, 1989; pp 53−108. (e) Brownridge, S.; Krossing, I.; Passmore, J.; Jenkins, H. D. B.; Roobottom, H. K. *Coord. Chem. Rev.* **2000**, *197*, 397−481. (f) Krossing, I. *Top. Curr. Chem.* **2003**, *230*, 135−152.

(8) Brownridge, S.; Cameron, T. S.; Passmore, J.; Schatte, G.; Way, T. C. *J. Chem. Soc., Dalton Trans.* **1996**, 2553−2570.

(9) (a) Kutney, G. W.; Turnbull, K. *Chem. Rev.* **1982**, *82*, 333−357. (b) Steudel, R.; Drozdova, Y.; Miaskiewicz, K.; Hertwig, R. H.; Koch, W. *J. Am. Chem. Soc.* **1997**, *119*, 1990−1996. (c) Zysman-Colman, E.; Harpp, D. N. *J. Sulfur. Chem.* **2004**, *25*, 291−316.

(10) (a) Passmore, J.; Sutherland, G. W.; Whidden, T. K.; White, P. S. *J. Chem. Soc., Chem. Commun.* **1980**, 289−290. (b) Murchie, M. P.; Johnson, J. P.; Passmore, J.; Sutherland, G. W.; Tajik, M.; Whidden, T. K.; White, P. S.; Grein, F. *Inorg. Chem.* **1992**, *31*, 273−283.

(11) Nenajdenko, V. G.; Shevchenko, N. E.; Balenkova, E. S.; Alabugin, I. V. *Chem. Rev.* **2003**, *103*, 229−282 and references therein.

upon addition of iodine.[10b] We therefore investigated the solutions by FT-Raman spectroscopy. We have also determined the stability of $S_2I_4^{2+}$ in all phases and accounted for the nonexistence of SI_3^+ in solution and the solid-phase on the basis of DFT calculations of the energetics, solvation energies, and lattice enthalpies. We show that $S_2I_4^{2+}$ and its multiple bonds are lattice stabilized in the solid state and in solutions of HSO_3F/AsF_5.

The previously reported X-ray structures of $S_2I_4(MF_6)_2$ were carried out at room temperature (rt), and the MF_6^- (M = As, Sb) anions were disordered in both cases and modeled with fixed M−F distances.[10] Herein, we report a low-temperature structure determination of $S_2I_4(AsF_6)_2$ with a higher accuracy.

In this paper, we focus on the experimentally based evidence (bond distances, stretching frequencies, and force constants) for the high S−S and I−I bond orders in $S_2I_4^{2+}$. In another publication, we will focus on the determination of S−S and I−I bond orders derived from theoretical calculations, as well as an analysis of the bonding in $S_2I_4^{2+}$, including AIM (atoms in molecules), NBO (natural bond orbital), and ELF (electron localization function) analyses. In addition, a study of various potential isomers of $S_2I_4^{2+}$ will be reported.

The ongoing discussion concerning multiple bonding between heavier main-group elements has, with exceptions,[1e] ignored the groups 16 and 17 elements. We hope the present contribution will help in rectifying this oversight.

2. Experimental Section

$S_2I_4(AsF_6)_2$ and $S_2I_4(SbF_6)_2$ were prepared according to literature methods from iodine (Aldrich, sublimed), sulfur (Fisher), and AsF_5 (Ozark-Mahoning) with SO_2 (Matheson, stored over CaH_2) as a solvent and using resublimed iodine, according to eqs 1 and 2.[10] Crystals of $S_2I_4(AsF_6)_2$ suitable for X-ray crystallography were formed by slow evaporation of the solvent SO_2 with a temperature gradient of 5 °C (+5 °C → 0 °C).

$$^1/_4S_8 + 2I_2 + 3AsF_5 \rightarrow S_2I_4(AsF_6)_2 + AsF_3 \quad (1)$$

$$^5/_4S_8 + 10I_2 + 18SbF_5 \rightarrow 5S_2I_4(SbF_6)_2 + 5SbF_3{\cdot}3SbF_5 \quad (2)$$

2.1. Vibrational Spectroscopy. FT-Raman spectra were measured on an FT-IR spectrometer (Bruker IFS66) equipped with an FT-Raman accessory (Bruker FRA106) using a Nd:YAG laser (emission wavelength, 1064 nm; maximum laser power, 300 mW). The data were collected in the backscattering mode (180° excitation; resolution, 4 or 2 cm^{-1}; apodization function, Norton−Beer, medium; zero filling factor, 2; acquisition mode, double-sided, fast return; scanner velocity, 4 mm/s; aperture, 12 mm) at rt or at 120 K. The low-temperature accessory (Bruker R495) consists of a glass cell that is mounted on a sample holder fitted with an *X*−*Y* translation stage. The glass cell is designed for use with 5-mm NMR tubes and has a vacuum shield that prevents condensation of moisture close to the measurement area. The sample tube is cooled by a stream of cold nitrogen gas, which is evaporated from a Dewar of liquid nitrogen using a rheostat-controlled immersion heater. The temperature of the sample is determined by the cooling rate of the evaporating nitrogen gas and was measured by a copper−constantan thermocouple (referenced with ice water) that was placed alongside the sample tube.

FT-Raman solution spectra in SO_2, AsF_3 (Ozark-Mahoning, stored over NaF), and HSO_3F (Aldrich, distilled) with an excess of AsF_5 and I_2, respectively, were measured using a reaction vessel incorporated with a 5-mm NMR tube. The 5-mm tube was long enough to be inserted into both the rt and low-temperature sample compartments of the FT-Raman attachment, allowing in situ preparation and adjustments to the solution concentration of samples by pouring an aliquot of the reaction mixture into the 5-mm tube. To obtain a spectrum that was not dominated by solvent peaks, it was necessary to concentrate the reaction solution until the solution became saturated and viscous. Concentration of the samples in HSO_3F was found to be unnecessary. An aliquot of the saturated solution was poured into the 5-mm tube, and an FT-Raman spectrum was acquired. A detailed description of the experiments is included in section 4 of the Supporting Information.

IR spectra were measured as neat solid samples between KBr plates on a Thermo Nicolet Nexus 470 FT-IR (32 scans; resolution, 2 cm^{-1}).

2.2. Normal-Coordinate Analysis. A DFT geometry optimization was accomplished with the help of the program system TURBOMOLE[12] using the DFT version of the DSCF module [functional B3-LYP,[13] basis sets of SV(P) quality] to aid in the determination of the force constants. The structural parameters are almost identical to those of the calculations presented in Table 2. The harmonic force field was numerically determined (NUMFORCE module). The more descriptive force constants were calculated in the system of internal or symmetry coordinates[14] by basis transformation[15] from the Cartesian force constants. The recalculation of the diagonal force constants on the basis of the experimentally deduced vibrational frequencies of the A_1 representation and the quantum chemically determined nondiagonal force constant elements was accomplished with the program FIT.[37] This routine also calculates the potential energy distribution in order to describe the motional form of a vibration with respect to the symmetry coordinates.

2.3. X-ray Crystallographic Analysis. The crystals were mostly twinned needles with a metallic blue-violet color. Only a few perfectly formed, square-based pyramids were found, and these were not twinned. A deep-purple, square-based pyramid crystal of $S_2I_4(AsF_6)_2$, having approximate dimensions of 0.23 × 0.23 × 0.18 mm, was mounted on a glass fiber and measured at −80 ± 1 °C on a mercury CCD area detector coupled with a Rigaku AFC8 diffractometer with graphite-monochromated Mo Kα radiation. The data were corrected for Lorentz polarization effects. A correction for absorption and secondary extinction was also applied. The structure was solved by direct methods.[16] All atoms were refined anisotropically.

2.4. Crystal data: $As_2F_{12}I_4S_2$, M = 949.56, monoclinic, space group = *C*2/*c* (No. 15), a = 9.605(2) Å, b = 12.734(2) Å, and c = 13.505(2) Å, β = 94.644(12)°, V = 1646.2(5) Å^3, Z = 4, μ(Mo Kα) = 119.20 cm^{-1}, 10 848 reflections measured, 4049 unique (R_{int}

(12) (a) Ahlrichs, R.; Bär, M.; Häser, M.; Horn, H.; Kölmel, C. *Chem. Phys. Lett.* **1989**, *162*, 165−169. (b) Eichkorn, K.; Treutler, O.; Öhm, H.; Häser, M.; Ahlrichs, R. *Chem. Phys. Lett.* **1995**, *240*, 283−289. (c) Eichkorn, K.; Treutler, O.; Öhm, H.; Häser, M.; Ahlrichs, R. *Chem. Phys. Lett.* **1995**, *242*, 652−660.

(13) (a) Becke, A. D. *Phys. Rev. A: At., Mol., Opt. Phys.* **1988**, *38*, 3098−3100. (b) Perdew, J. P. *Phys. Rev. B: Condens. Matter* **1986**, *33*, 8822−8824. (c) Treutler, O.; Ahlrichs, R. *J. Chem. Phys.* **1995**, *102*, 346−354.

(14) Wilson, E. B.; Decius, J. C.; Cross, P. C. *Molecular Vibrations, The Theory of Infrared and Raman Vibrational Spectra*; McGraw-Hill: New York, 1955.

Table 2. Selected Experimental and Calculated Bond Lengths [Å] and Angles [deg] for $S_2I_4^{2+}$

	$S_2I_4^{2+}(AsF_6)_2$ (this work)	$S_2I_4^{2+}(AsF_6)_2$[10]	$S_2I_4^{2+}(SbF_6)_2$[10]	calcd C_2 (PBE0/SDB-cc-pVTZ)	calcd C_{2v} (PBE0/SDB-cc-pVTZ)	calcd C_{2v} CCSD/SBD-cc-pVTZ
T [°C]	−80	25	25			
S−S	1.842(4)	1.843(6)	1.818(10)	1.857	1.847	1.852
I1−I2	2.6026(9)	2.5987(15)	2.571(2)	2.613	2.608	2.625
I1−S	2.827(2)	2.860(4)	2.993(4)	2.861	3.077	3.085
I2−S	3.216(2)	3.178(4)	2.993(4)	3.349	3.077	3.085
I−S−I	88.76(4)	89.43(11)	90.38(16)	106.5[a]	106.9[a]	101.5[a]
I−I−S	88.03(5)/76.95(4)	87.11(7)/78.56(7)	82.77(10)	89.3/76.7	82.9	82.8
I−S−S	101.85(11)/92.51(11)	100.96(19)/93.35(19)	97.23(19)	103.0/90.8	97.1	97.20
I1−S−S−I1	90.51(11)	89.8(1)	91.3(1)	104.0[a]	108.1[a]	102.7[a]
I2−I1−S−S	−1.62(9)	−1.2(1)	0	−3.5	0	0

[a] The structure restrained to an I−S−I dihedral angle of 90° is only 8 kJ/mol (PBE0/SDB-cc-pVTZ) higher in energy (see also Figure 9 in the Supporting Information). The larger calculated I−S−I and I1−S−S−I1 angles arise from repulsion between the partially charged diiodine units and the low potential energy surface. In addition, the larger calculated angles might be due to the inability of calculation methods used to describe the dispersion forces correctly.[61]

= 0.029), GOF = 1.690. The final cycle of full-matrix least-squares refinement on F was based on a total of 1966 observed reflections [$I > 3.00\sigma(I)$] and 121 variable parameters and was converged with unweighted and weighted agreement factors of $R = \sum||F_o| - |F_c||/\sum|F_o| = 0.035$ and $R_w = [\sum w(|F_o| - |F_c|)^2/\sum wF_o^2]^{1/2} = 0.041$.

2.5. Computational Details. All DFT calculations (except the normal-coordinate analysis), including the geometry optimizations, and frequency and energy calculations were carried out using the GAUSSIAN 98[17] and GAUSSIAN 03[18] suite of programs. The MOLPRO[19] program package was employed in coupled cluster calculations. The pictorial descriptions of the calculated normal modes were obtained with MOLDA[20] and HYPERCHEM[21] and were assigned from these visualizations.

Various levels of theory have been used to reproduce the observed geometries of $S_2I_4^{2+}$. (The calculated geometries using different methods and different basis sets are included in Table 2 of the Supporting Information.) Ab initio methods failed to reproduce the observed structure: Hartree−Fock and second-order Møller−Plesset correlation methods did not find a stationary point on the potential energy surface starting from the experimental geometry. The one-parameter hybrid functional with a modified Perdew−Wang exchange and correlation (MPW1PW91)[22] and the parameter-free hybrid functional of Perdew−Burke−Ernzerhof (PBE0)[23] were used in DFT calculations. The MPW1PW91 functional has been shown to predict the geometries of sulfur homopolyatomic species (e.g., S_8^{2+} and S_4^{2+})[24] and iodine homopolyatomic cations[7e] in reasonable agreement with the experimental geometries. The PBE0 functional was recently shown to perform well in predicting the molecular properties of small selenium halogen cations.[25]

Basis sets used in the calculations included the all-electron (AE) basis sets 3-21G* and 6-311G*[26] and the effective core potential (ECP) basis set SDB-cc-pVTZ.[27] The 6-311G* basis set was augmented with appropriate numbers of d and f polarization functions and s and p diffuse functions for energy calculations. The SDB-cc-pVTZ basis set employed Dunning's correlation-consistent basis set for sulfur and quasi-relativistic energy-adjusted ECP of the Stuttgart group combined with the correlation-consistent valence basis set of Martin and Sundermann for iodine.[27]

The vibrational frequencies were calculated by all methods and are only in approximate agreement, and some calculations gave one imaginary frequency. The match of calculated and experimental

(15) Pulay, P. Program for Transformation of Force Constants FCT, Fayetteville, AR.

(16) Sheldrick, G. M. *SHELX-97 Programs for Crystal Structure Analysis (Release 97-2)*; Institut für Anorganische Chemie der Universität Göttingen: Göttingen, Germany, 1997.

(17) Frisch, M. J.; Trucks, G. W.; Schlegel, H. B.; Scuseria, G. E.; Robb, M. A.; Cheeseman, J. R.; Zakrzewski, V. G.; Montgomery, J. A., Jr.; Stratmann, R. E.; Burant, J. C.; Dapprich, S.; Millam, J. M.; Daniels, A. D.; Kudin, K. N.; Strain, M. C.; Farkas, O.; Tomasi, J.; Barone, V.; Cossi, M.; Cammi, R.; Mennucci, B.; Pomelli, C.; Adamo, C.; Clifford, S.; Ochterski, J.; Petersson, G. A.; Ayala, P. Y.; Cui, Q.; Morokuma, K.; Salvador, P.; Dannenberg, J. J.; Malick, D. K.; Rabuck, A. D.; Raghavachari, K.; Foresman, J. B.; Cioslowski, J.; Ortiz, J. V.; Baboul, A. G.; Stefanov, B. B.; Liu, G.; Liashenko, A.; Piskorz, P.; Komaromi, I.; Gomperts, R.; Martin, R. L.; Fox, D. J.; Keith, T.; Al-Laham, M. A.; Peng, C. Y.; Nanayakkara, A.; Challacombe, M.; Gill, P. M. W.; Johnson, B.; Chen, W.; Wong, M. W.; Andres, J. L.; Gonzalez, C.; Head-Gordon, M.; Replogle, E. S.; Pople, J. A. *Gaussian 98*, Revision A.11; Gaussian, Inc.: Pittsburgh, PA, 2001.

(18) Frisch, M. J.; Trucks, G. W.; Schlegel, H. B.; Scuseria, G. E.; Robb, M. A.; Cheeseman, J. R.; Montgomery, J. A., Jr.; Vreven, T.; Kudin, K. N.; Burant, J. C.; Millam, J. M.; Iyengar, S. S.; Tomasi, J.; Barone, V.; Mennucci, B.; Cossi, M.; Scalmani, G.; Rega, N.; Petersson, G. A.; Nakatsuji, H.; Hada, M.; Ehara, M.; Toyota, K.; Fukuda, R.; Hasegawa, J.; Ishida, M.; Nakajima, T.; Honda, Y.; Kitao, O.; Nakai, H.; Klene, M.; Li, X.; Knox, J. E.; Hratchian, H. P.; Cross, J. B.; Adamo, C.; Jaramillo, J.; Gomperts, R.; Stratmann, R. E.; Yazyev, O.; Austin, A. J.; Cammi, R.; Pomelli, C.; Ochterski, J. W.; Ayala, P. Y.; Morokuma, K.; Voth, G. A.; Salvador, P.; Dannenberg, J. J.; Zakrzewski, V. G.; Dapprich, S.; Daniels, A. D.; Strain, M. C.; Farkas, O.; Malick, D. K.; Rabuck, A. D.; Raghavachari, K.; Foresman, J. B.; Ortiz, J. V.; Cui, Q.; Baboul, A. G.; Clifford, S.; Cioslowski, J.; Stefanov, B. B.; Liu, G.; Liashenko, A.; Piskorz, P.; Komaromi, I.; Martin, R. L.; Fox, D. J.; Keith, T.; Al-Laham, M. A.; Peng, C. Y.; Nanayakkara, A.; Challacombe, M.; Gill, P. M. W.; Johnson, B.; Chen, W.; Wong, M. W.; Gonzalez, C.; Pople, J. A. *Gaussian 03*, Revision B.05; Gaussian, Inc.: Pittsburgh, PA, 2003.

(19) Amos, R. D.; Bernhardsson, A.; Berning, A.; Celani, P.; Cooper, D. L.; Deegan, M. J. O.; Dobbyn, A. J.; Eckert, F.; Hampel, C.; Hetzer, G.; Knowles, P. J.; Korona, T.; Lindh, R.; Lloyd, A. W.; McNicholas, S. J.; Manby, F. R.; Meyer, W.; Mura, M. E.; Nicklass, A.; Palmieri, P.; Pitzer, R.; Rauhut, G.; Schütz, M.; Schumann, U.; Stoll, H.; Stone, A. J.; Tarroni, R.; Thorsteinsson, T.; Werner, H.-J. *MOLPRO*.

(20) Yoshida, H.; Matsuura, H. *J. Chem. Software* **1997**, *3*, 147.

(21) *HYPERCHEM 3.0*; Hypercube, Inc.: Gainesville, FL, 1993.

(22) (a) Adamo, C.; Barone, V. *Chem. Phys. Lett.* **1997**, *274*, 242−250. (b) Adamo, C.; Barone, V. *J. Chem. Phys.* **1998**, *108*, 664−675.

(23) (a) Perdew, J. P.; Burke, K.; Ernzerhof, M. *Phys. Rev. Lett.* **1996**, *77*, 3865−3868. (b) Perdew, J. P.; Burke, K.; Ernzerhof, M. *Phys. Rev. Lett.* **1997**, *78*, 1396. (c) Perdew, J. P.; Ernzerhof, M.; Burke, K. *J. Chem. Phys.* **1996**, *105*, 9982−9985. (d) Adamo, C.; Barone, V. *J. Chem. Phys.* **1999**, *110*, 6158−6170.

(24) (a) Cameron, T. S.; Deeth, R. J.; Dionne, I.; Du, H.; Jenkins, H. D. B.; Krossing, I.; Passmore, J.; Roobottom, H. K. *Inorg. Chem.* **2000**, *39*, 5614−5631. (b) Krossing, I.; Passmore, J. *Inorg. Chem.* **1999**, *38*, 5203−5211 and references therein. (c) Jenkins, H. D. B.; Jitariu, L. C.; Krossing, I.; Passmore, J.; Suontamo, R. *J. Comput. Chem.* **2000**, *21*, 218−226.

(25) Rautiainen, J. M.; Way, T.; Schatte, G.; Passmore, J.; Laitinen, R. S.; Suontamo, R. J.; Valkonen, J. In press.

(26) Glukhovtsev, M. N.; Pross, A.; McGrath, M. P.; Radom, L. *J. Chem. Phys.* **1995**, *103*, 1878−1885.

(27) (a) Martin, J. M. L.; Sundermann, A. *J. Chem. Phys.* **2001**, *114*, 3408−3420. (b) Woon, D. E.; Dunning, T. H., Jr. *J. Chem. Phys.* **1993**, *83*, 1358−1371. (c) Bergner, A.; Dolg, M.; Kuechle, W.; Stoll, H.; Preuss, H. *Mol. Phys.* **1993**, *80*, 1431−1441.

Table 3. Observed (FT-Raman) and Calculated[a] (PBE0/SDB-cc-pVTZ) Vibration Frequencies [cm^{-1}] and Intensities for $S_2I_4^{2+}$

$S_2I_4^{2+}$ (C_2) in $S_2I_4(AsF_6)_2$	$S_2I_4^{2+}$ (C_{2v}) in $S_2I_4(SbF_6)_2$	$S_2I_4^{2+}$ calcd C_2 (IR/Raman)	$S_2I_4^{2+}$ calcd C_{2v} (IR/Raman)	calcd (C_{2v}) vibrational modes[b] and symmetry	assignments[b]
734 (w)/IR: 738 (m)	732 (w)/IR: 737 (m)	760 (100/45)	786 (100/80)	$\nu_1(A_1)$	ν_s(S−S)
228 (s)	227 (m)	242 (3/46)	245 (3/50)	$\nu_2(A_1)$	ν_s(I−I)
166 (vs)	166 (vs)	141 (15/100)	141 (14/100)	$\nu_3(A_1)$	$\nu(S_2I_4, A_1)$
		27 (0/5)	26 (1/41)	$\nu_4(A_1)$	scissor
207 (s)		198 (2/72)	187 (0/28)	$\nu_5(A_2)$	$\nu(S_2I_4, A_2)$
		37 (0/33)	31 (0/8)	$\nu_6(A_2)$	deformation
		22 (0/15)	−22 (0/2)	$\nu_7(A_2)$	deformation
		242 (9/1)	244 (10/0)	$\nu_8(B_1)$	ν_{as}(I−I)
178 (s)	179 (sh)	166 (82/41)	159 (76/41)	$\nu_9(B_1)$	$\nu(S_2I_4, B_1)$
		218 (10/23)[c]	215 (4/19)[c]	$\nu_{10}(B_2)$	$\nu(S_2I_4, B_2)$
		90 (4/4)	94 (8/2)	$\nu_{11}(B_2)$	deformation
		33 (0/3)	35 (0/3)	$\nu_{12}(B_2)$	deformation

[a] The calculated frequencies are unscaled. [b] A visualization of the vibrational modes is included in Figure 6 of the Supporting Information. [c] We note that ν_{10} is not observed. The calculated Raman intensities are smaller than that calculated for ν_5 in C_{2v} $S_2I_4^{2+}$, which was not observed for $S_2I_4(SbF_6)_2$.

Raman intensities was not good, which is often the case. (The PBE0/SDB-cc-pVTZ results are included in Table 3, and the others are included in Table 2 of the Supporting Information.)

The method and the basis set used have a strong effect on the energies. Previous calculations for the dissociation energy of S_4^{2+} into $2S_2^+$ show a strong dependence on the size of the basis set and the correlation method used.[24b,c] Hybrid HF/DFT (B3PW91/6-311+G(3df)//B3PW91/6-311+G*) methods were found to be sufficient to describe the energetics of this system, though some difficulties in calculating the first ionization potential of S_2 still exist (calculated, 925.2 kJ; experimental, 902.7 kJ/mol).[24b,c] In this work, the MPW1PW91 method was employed to describe the $S_2I_4^{2+}$ system. At this level, the calculated reaction enthalpies of S_4^{2+} to give $2S_2^+$ are −348, −312, and −254 kJ/mol with the basis sets of 3-21G*, 6-311+G*, and 6-311+G(3df)//6-311+G*, respectively (cf. −256 kJ/mol for B3PW91/6-311+G(3df)//6-311+G*). This also implied that 3-21G* is not sufficient to describe the energetics of sulfur- and iodine-containing[28] molecules. Therefore, these calculations are qualitative rather than quantitative, and in some cases, one could arrive at an erroneous conclusion. The calculated reaction enthalpies for the reaction of $S_2I_4^{2+}$ and I_2 giving $2SI_3^+$ decreases from −206 to −285 kJ/mol when going from MPW1PW91/3-21G* to the higher CCSD(T)/SDB-cc-pVTZ level. However, using the latter does not improve the calculated geometries, vibrational frequencies, and Raman intensities.

The solvation energies were calculated using a polarization continuum model (PCM) with the integral equation formalism (IEF)[29] incorporated in G03W (B.05). The following parameters were used to describe the solvent. SO_2: dielectric constant = 14.0, solvent radius (R_{solv}) = 2.021 Å, molar volume (V_{mol}) = 46.75 Å^3, numeral density = 0.012 88 Å^{-3}, density = 1.370 27 g/mL. HSO_3F: dielectric constant = 120.0, solvent radius (R_{solv}) = 2.21 Å, molar volume (V_{mol}) = 57.98 Å^3, numeral density = 0.010 39 Å^{-3}, density = 1.726. The solvent radii were obtained by regression of $R_{solv}(x)$ calculated from molar volume and $R_{solv}(y)$ of known solvents in G03W ($y = 0.9254x - 0.4206$, regression coefficient $R^2 = 0.9926$).

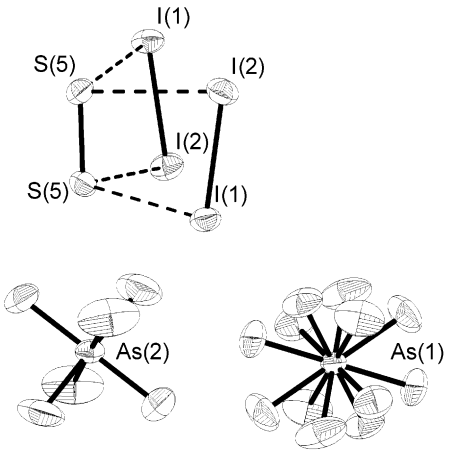

Figure 1. Structure of the $S_2I_4^{2+}$ cation and two AsF_6^- anions. Thermal ellipsoids are drawn at 50% probability.

3. Results and Discussion

3.1. Structure of $S_2I_4^{2+}$ in $S_2I_4(AsF_6)_2$. 3.1.1. X-ray Structure of $S_2I_4(AsF_6)_2$. Single crystals of $S_2I_4(AsF_6)_2$ of good quality were prepared in this work, and the structure has been reexamined at low temperature (−80 °C) in order to obtain a more accurate structure with correctly modeled AsF_6^- anions. The structure of $S_2I_4^{2+}$ is shown in Figure 1, and corresponding parameters are given in Table 2. The crucial S−S and I−I bond lengths were determined to be 1.842(4) and 2.6026(9) Å, respectively [1.843(6) and 2.5987(15) Å, respectively, in the previously reported structure],[10] with corresponding Pauling bond orders[30] of 2.4 for the S−S bond and 1.3 for the I−I bond. The very long S−I bonds correspond to bond orders of 0.15 and 0.03, indicating the very weak S−I interaction. In the previously reported structure determination (at rt) of $S_2I_4(AsF_6)_2$ and $S_2I_4(SbF_6)_2$, the $S_2I_4^{2+}$ cations consisted of a distorted right-triangular prism (C_2; AsF_6^- case) or a right-triangular prism (C_{2v}; SbF_6^- case), respectively (see Figure 2).

(28) According to the experimental observations that $I_4(AsF_6)_2$ is formed instead of $I_2(AsF_6)$, and $I_2(Sb_2F_{11})$ instead of $I_4(Sb_2F_{11})_2$, Jenkins et al. estimated that the dissociation enthalpies of I_4^{2+} to give $2I_2^+$ are between −413 and −463 kJ/mol.[45] However, the calculated enthalpies using different methods and basis sets gave much lower values, between −250 and −316 kJ/mol (see footnote of Table 4). This is a cautionary note when conclusions are drawn based upon these calculated energies.

(29) (a) Cancès, E.; Mennucci, B.; Tomasi, J. *J. Chem. Phys.* **1997**, *107*, 3032−3041. (b) Cossi, M.; Barone, V.; Mennucci, B.; Tomasi, J. *Chem. Phys. Lett.* **1998**, *286*, 253−260.

(30) Estimated by using a modified Pauling equation, as described in ref 10.

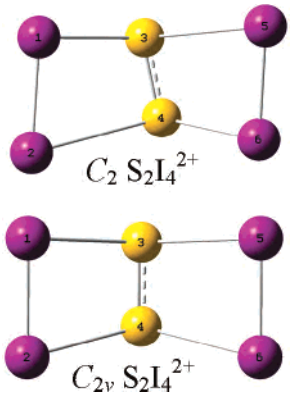

Figure 2. Visualization of the calculated (MPW1PW91/6-311+G*) structures of C_2 and C_{2v} $S_2I_4^{2+}$.

The $S_2I_4^{2+}$ in $S_2I_4(AsF_6)_2$ has C_2 symmetry and is more distorted than previously reported, while the S−S and I−I bond lengths are almost identical in both cases. Two planar S_2I_2 units [I2−I1−S−S torsion angle of −1.62(9)°], joined by an S−S bond, form a distorted right-triangular prism (Figure 1). The distortion of the $S_2I_4^{2+}$ cation from C_{2v} symmetry arises from the differences in S−I bond lengths [cf. S−I1 2.827(2), S−I2 3.216(2) Å in this structure with S−I1 2.860(4), S−I2 3.178(4) Å in the previous structure of the AsF_6^- salt[10]], which are longer in this structure. This results in a larger tilt of the I−I units with respect to the S−S axis. The distortion of these weak S−I bonds may arise from the cation−anion interaction, which, in this structure, we can now estimate (see below). We note that the difference in the distortion in the two structures may arise from the different temperatures of the structure determinations, that is, rt (previous study)[10] and −80 °C (this work).

There are at least five fluorine contacts for each I1 atom and three for each I2 atom, which are below the sum of their van der Waals distance of 3.45 Å[31] (Figure 3). As a result, there are higher formal charges residing on the I2 atom (+0.39) than on the I1 atom (+0.27), as estimated according to Pauling's electrostatic valence rule by the method of Brown (Figure 4).[32] Each sulfur atom has four contacts to three different anions, leading to an estimated charge of 0.22. The experimentally based charges are in agreement with our simple bonding model (Figure 5),[10] in which there is equal distribution of the positive charge over the S_2 and two I_2 units (0.33 on each atom).

The positions of the AsF_6^- anions in $S_2I_4(AsF_6)_2$ were well-determined at low temperature. There are two crystallographically different AsF_6^- anions (Figure 1), one ordered and one disordered (74:26). The As−F bond lengths range from 1.65(2) to 1.721(7) Å, with an average of 1.695(14) Å for $As1F_6^-$ (disordered) and 1.704(6) Å for $As2F_6^-$ (ordered). The F−As−F bond angles deviate by less than 2.2° from 90°. All of the fluorine atoms exhibit at least one contact with iodine or sulfur atoms within the sum of the van der Waals radii. The sums of the F···S and F···I valence units (Figure 4) imply a formal charge of −0.97 on $As1F_6^-$ and −0.78 on $As2F_6^-$, which are within expectations (detailed figures of the surroundings of the cation and the two different anions are given in Figures 1−3 of the Supporting Information).

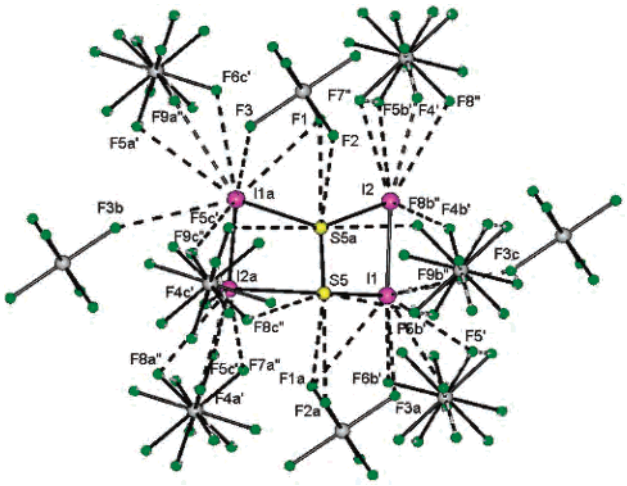

Figure 3. I···F and S···F contacts in $S_2I_4(AsF_6)_2$ are less than the sum of their van de Waals distances of 3.45 and 3.20 Å, respectively. Contacts (in Å): I1a···F1 3.275(8), I1a···F3b 3.378(6), I1a···F3 3.137(8), I1a···F5a′ 3.361(8), I1a···F6c′ 3.246(8), I1a···F9a″ 3.18(3), I1···F9c″ 3.33(2), I2···F4′ 2.964(9), I2···F4b′ 3.392(7), I2···F5b′ 3.371(9), I2···F7″ 3.06(2), I2···F8″ 3.32(3), S5a···F1 3.041(7), S5a···F2 3.094(7), S5a···F5c′ 3.174(8), S5a···F8b″ 2.95(2). Symmetric operations: *a* (−*x*, *y*, 0.5 − *z*), *b* (−*x*, −*y*, −*z*), *c* (*x*, −*y*, 0.5 + *z*).

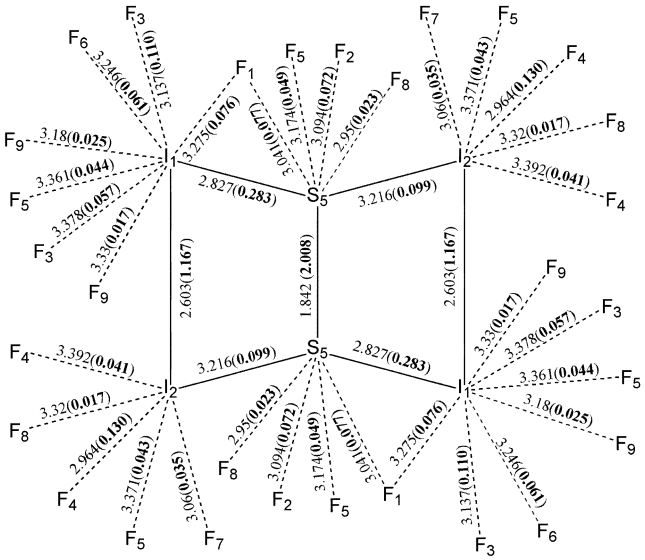

Figure 4. Bond valence map of $S_2I_4^{2+}$ unit showing S···F and I···F contacts below their van de Waals distance of 3.20 and 3.45 Å, respectively (distances in Å). The bond valences in parentheses and in bold have taken account of the occupancies of the fluorine atoms by multiplying the occupancies. The calculated atomic valences are 1.72 (I1), 1.66 (I2), and 2.61 (S5), and the calculated formal charges are +0.39 (I1), +0.27 (I2), and +0.22 (S5), with a total charge of +1.75 on the $S_2I_4^{2+}$ unit.

3.1.2. Calculation of the Geometry of $S_2I_4^{2+}$. Calculations starting from experimental structures at Hartree−Fock

(31) Bondi, A. *J. Chem. Phys.* **1964**, *68*, 441−451.

(32) The contacts *S* have been defined as $S = (R/R_0)^{-N}$ or $S = \exp[(R_0 - R)/B]$, where *R* is the observed distance, R_0 is the value of the bond length with the unit bond valence, and *N* and *B* are constants. Used constants: S···F, $N = 3.80$, $R_0 = 1.55$; I···F, $R_0 = 2.32$, $B = 0.37$; S−I, $R_0 = 2.36$, $B = 0.37$; I−I, $R_0 = 2.66$, $B = 0.37$; S−S, $R_0 = 2.10$, $B = 0.37$; As−F, $R_0 = 1.62$, $B = 0.37$. The constants are available from http://ccp14.sims.nrc.ca/ccp/web-mirrors/i_d_brown/bond_valence_param/, or see Brown, I. D. *The Chemical Bond in Inorganic Chemistry—The Bond Valence Model*; Oxford University Press: Oxford, U.K., 2002.

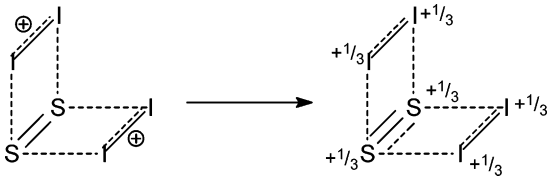

Figure 5. S_2 is interacting with two I_2^+ in two mutually perpendicular planes via the unpaired electrons donating in π^* orbitals of each I_2^+. The equal distribution of charge on all atoms [the ionization energies of S_2(g) (9.40 ± 0.05 eV) and I_2(g) (9.39 ± 0.10 eV) are essentially the same][62] leads to an S−S bond order of 2.33, an I−I bond order of 1.33, a $+^1/_3$ charge on all atoms, and a $+^2/_3$ charge on each dimer.[10b]

and second-order Møller−Plesset perturbation theory levels failed to produce the observed structures. DFT optimizations using C_{2v} symmetry constraints led to structures that were in reasonable agreement with experimental structures, and subsequent CCSD optimization did not improve this agreement. However, all frequency calculations done with triple-valence ζ-quality basis sets gave an imaginary frequency for the ν_7 deformation normal mode, indicating that the C_{2v} stationary point was a saddle point. DFT reoptimization in lower C_2 symmetry gave a true minimum structure 1 kJ/mol lower in energy. The small energy difference between the structures (Figure 2) suggests that the potential energy surface around the minimum is shallow and the structure is readily distorted. The calculated geometries are in very good agreement with the experimental geometries in the solid-state structures [AsF_6^- (C_2), SbF_6^- (C_{2v}); Table 2]. Attempts to optimize the C_2-symmetric species with the CCSD method did not produce the experimentally observed structure. This was most probably due to the inability of the Hartree−Fock reference to describe this weakly bound system. The geometry calculated with the SDB-cc-pVTZ basis set is given in Table 2, and AE results can be found in section 5 of the Supporting Information.

The presence of iodine atoms in the $S_2I_4^{2+}$ cation called for consideration of relativistic effects in the calculations. Relativistic effects were included in the calculations in an approximate way by using a relativistic ECP basis set. Inclusion of relativistic effects was expected to weaken the bonds compared to nonrelativistic AE calculations.[33] However, the bonds predicted by the SDB-cc-pVTZ basis set were shorter than the bonds calculated with AE basis sets. Despite this fact, structures predicted with the SDB-cc-pVTZ basis set gave the best agreement with experimental structures because all calculated bond lengths were longer than observed bonds. The better performance of the SDB-cc-pVTZ basis sets is expected to arise from the better quality of the valence basis set compared with that of the AE basis sets used. The deviations between calculated and observed structures are attributed to the incompleteness of the basis set used[33a] and to the shallow nature of the potential energy surface around the minimum, which allows the structure to be easily distorted from the gas-phase minimum (Figure 9 of the Supporting Information).

(33) (a) Visscher, L.; Dyall, K. G. *J. Chem. Phys.* **1996**, *104*, 9040−9046. (b) Visscher, L.; Styszynski, J.; Nieuwpoort, W. C. *J. Chem. Phys.* **1996**, *105*, 1987−1994. (c) de Jong, W. A.; Styszynski, J.; Visscher, L.; Nieuwpoort, W. C. *J. Chem. Phys.* **1998**, *108*, 5177−5184.

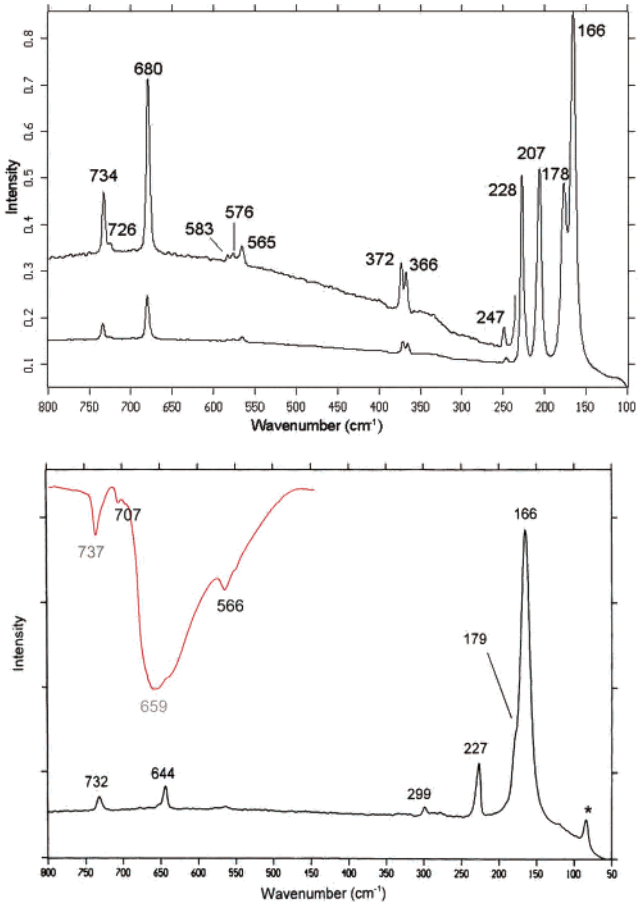

Figure 6. (a) FT-Raman spectrum of $S_2I_4(AsF_6)_2$ (laser power 25 mW, resolution 2 cm^{-1}, 512 scans, T = 120 K) and (b) FT-Raman (laser power 22 mW, resolution 2 cm^{-1}, 2048 scans, T = 150 K) and IR (neat solid between KBr plates, baseline corrected) spectra of $S_2I_4(SbF_6)_2$. The peak marked with an asterisk is due to glass.

3.2. Vibrational Spectroscopy. 3.2.1. FT-Raman and IR Spectra. The FT-Raman and IR spectra of $S_2I_4(SbF_6)_2$(s) and the FT-Raman spectrum of $S_2I_4(AsF_6)_2$(s) are shown in Figure 6. Table 3 lists the observed and calculated (PBE0/SDB-cc-pVTZ corresponding to the best calculated geometries) vibrational frequencies, intensities, and assignments. The experimental frequencies are in agreement with the calculated values, while the intensities, as is usually the case, are in rough agreement. The S−S stretch is clearly observed in the FT-Raman [734 (AsF_6^- salt) and 732 cm^{-1} (SbF_6^- salt)] and IR spectra [738 (AsF_6^-) and 737 cm^{-1}(SbF_6^-)]. Similar symmetric S−S stretches have been observed in S_2(g) (700 cm^{-1}) and S_2^+(g) (790 cm^{-1}), which have bond orders of 2.0 and 2.5, respectively, implying an S−S bond order of 2.2 in $S_2I_4^{2+}$ (a detailed discussion is included with the Supporting Information). The observed weak peak at 247 cm^{-1} in the FT-Raman spectra of the AsF_6^- salt has not been unequivocally assigned; it could be either a combination mode or an impurity. The I−I stretches are assigned to the peaks at 228/227 cm^{-1} and correspond to an I−I bond order of 1.3. Although the calculated I−I stretches occur at higher wavenumbers, the assignment is reasonable because, compared to other iodine cations, the I−I stretch is expected at a lower frequency than in I_2^+ [238 cm^{-1} (exptl), 255 cm^{-1} (calcd)]. The most intense peak, at 166 cm^{-1}, is attributed

to the symmetric S−I stretch. The asymmetric S−I stretch is found at a slightly higher wavenumber, 178 cm^{-1}.[34] Both S−I stretches are calculated at lower frequencies than those of the detected peaks, and this is connected to the underestimated S−I bond strengths by the present calculations. The observed peak at 207 cm^{-1} in $S_2I_4(AsF_6)_2$ has been tentatively assigned to an S−S deformation mode (ν_5). In comparison, the ν_5 normal mode in the spectrum of the SbF_6^- salt is either absent or very weak. The absence of the ν_5 mode in the spectrum of $S_2I_4(SbF_6)_2$ is related to the higher symmetry of $S_2I_4^{2+}$ (C_{2v}) in the SbF_6^- salt. Calculated Raman spectra support this conclusion because the ν_5 mode has a considerably smaller calculated relative Raman activity for C_{2v}-symmetric species than for C_2-symmetric species. Consistent with the higher symmetry of $S_2I_4^{2+}$ (C_2 in the AsF_6^- salt and C_{2v} in the SbF_6^- salt), there are fewer peaks in the spectrum of the SbF_6^- salt. The S−S and I−I stretching frequencies are almost identical in the two compounds, implying that the bond distances are also. This conclusion could not be drawn from the X-ray crystal structures. The peaks at 680 (ν_1), 563−583 (ν_2), and 366−372 (ν_5) cm^{-1} are due to the AsF_6^- anions, and the peaks at 644 (ν_1) and 298 (ν_5) cm^{-1} are due to SbF_6^-.[35]

3.2.2. Normal-Coordinate Analysis. A bond order determined from the observed vibrational spectra is only valid if the vibration only involves the two atoms in question. To remove all doubts concerning the possible mixing of vibrations, we extended the experimental findings (Raman frequencies) by a normal-coordinate analysis. It has been shown that the force constant matrices of small molecules calculated by means of ab initio or DFT methods (i.e., H_2GaCl)[36] agree well with those derived from experimental investigations. This particularly applies to the nondiagonal elements F_{ij} ($i \neq j$), which are a measure for the interaction of the vibrations of an irreducible representation. The advantage of a normal-coordinate analysis lies in the fact that the force constant values of the bonds can be determined properly even if coupling between the modes within an irreducible representation exists.

The 12 normal modes for the C_{2v} $S_2I_4^{2+}$ are of A_1 (4), A_2 (3), B_1 (2), and B_2 (3) symmetry (Table 3). After transformation of the force constant matrix in Cartesian coordinates (obtained by chemical methods) into the system of symmetry coordinates {$S_1 = r$(S−S), $S_2 = (1/2)^{1/2}[r_1$(I−I) + r_2(I−I)], $S_3 = (1/2)[r_1$(S−I) + r_2(S−I) + r_3(S−I) + r_4(S−I)], $S_4 = (1/2)^{1/2}[r_1$(I···I) + r_2(I···I)]}, the following force constant matrix (in mdyn/Å) in the totally symmetric irreducible representation A_1 (calculated frequencies 749.1, 228.5, 123.2, and 25.6 cm^{-1}) was obtained:

$$F_{11} = 5.29, \quad F_{22} = 1.97, \quad F_{33} = 0.36, \quad F_{44} = 0.04,$$
$$F_{12} = 0.10, \quad F_{13} = 0.05, \quad F_{14} = -0.02, \quad F_{23} = -0.05,$$
$$F_{24} = 0.01, \quad F_{34} = -0.05$$

F_{11} and F_{22} correspond to the S−S and symmetrical I−I force constants, respectively. Recalculation of the diagonal elements of the force constant matrix, while keeping the nondiagonal elements constant and replacing the frequencies by the observed values (734.0, 228.0, and a completely symmetric S−I mode within the range of 100−170 cm^{-1}), leads to the following diagonal force constants:

$$F_{11} = 5.078 \pm 0.002, \quad F_{22} = 1.950 \pm 0.001,$$
$$F_{33} = 0.438 \pm 0.146, \quad F_{44} = 0.034 \pm 0.001$$

From the calculation of the potential energy distribution, we conclude that all of the vibrational modes in the A_1 representation are pure, unmixed vibrations.[37] This is confirmed by the calculations of the B_1 representation {symhfmetry coordinates $S_8 = (1/2)^{1/2}[r_1$(I−I) − r_2(I−I)], $S_9 = (1/2)[r_1$(S−I) + r_2(S−I) − r_3(S−I) − r_4(S−I)]} resulting in an almost identical value for the diagonal force constant F_{88} = 1.94 mdyn/Å for the "anti"symmetric I−I vibration. Therefore, one can assume that no vibrational coupling exists between the I−I bonds.

To evaluate the bond order of the bonds in $S_2I_4^{2+}$, we compare the experimental force constants for $S_2I_4^{2+}$ with the experimentally deduced force constants of the related compounds S_2(g), S_2^+(g), I_2(g), and I_2^+(g), as well as those of matrix-isolated FSSF and SSF_2,[38] because these parameters are directly correlated to the gradient of the potential energy close to the equilibrium bond distance.[39] The valence force constants are determined to be 4.89 [S_2(g)],[40] 5.88 [S_2^+(g)],[40] 5.10 [SSF_2(g)],[38] 3.47 [FSSF(g)],[38] 1.72 [I_2(g)],[40] and 2.15 [I_2^+(g)] mdyn/Å.[40]

Assuming that the experimental force constants are directly related to the bond order (see section 6 of the Supporting Information), the S−S bond order in $S_2I_4^{2+}$ is estimated to be about 2.2 and the I−I force constant corresponds to an I−I bond order of about 1.3. These bond orders are in appropriate agreement with those predicted by our simple model (2.33 for S−S and 1.33 for I−I; see Figure 5).[10] For multiple bonds between atoms of the second row of the periodic table, the force constants are directly correlated to the bond order (e.g., the double-bond force constant is twice that of the single bond and a triple-bond force constant is 3 times that of a single bond). Similar estimates of the force

(34) The peaks present, to a lesser or greater extent, at 178 (m) and 190 (vw) cm^{-1} might be due to elemental iodine [I_2(s): 180 (s), 190 (w) cm^{-1}]. Nevertheless, the absence of the weak peak at 190 cm^{-1} (B_{3g} stretching mode of solid I_2; Anderson, A.; Sun, T. S. *Chem. Phys. Lett.* **1970**, *6*, 611−616) in some spectra and the slight shift of the peak from 178 to 180 cm^{-1} in spectra where elemental iodine is undoubtedly present lead to the conclusion that the iodine peak, where present, overlaps with a vibration due to $S_2I_4^{2+}$.

(35) The splitting of ν_2 and ν_5 of the AsF_6^- peaks in the well-resolved Raman spectrum of $S_2I_4(AsF_6)_2$ is consistent with the presence of more than one crystallographically different AsF_6^- anion that are slightly distorted from O_h symmetry.

(36) Köppe, R.; Schnöckel, H. *J. Chem. Soc., Dalton Trans.* **1992**, 2293−3395.

(37) Becher, H.-J.; Mattes, R. *Spectrochim. Acta, Part A* **1969**, *23A*, 2449−2451.

(38) Haas, A.; Willner, H. *Spectrochim. Acta, Part A* **1979**, *35A*, 953−959 and references therein.

(39) Köppe, R.; Schnöckel, H. *Z. Anorg. Allg. Chem.* **2000**, *626*, 1095−1099.

(40) Huber, K. P.; Herzberg, G. Constants of Diatomic Molecules (data prepared by J. W. Gallagher and R.D. Johnson, III). In *NIST Chemistry WebBook*; Linstrom, P. J., Mallard, W. G., Eds.; NIST Standard Reference Database Number 69; National Institute of Standards and Technology: Gaithersburg, MD, 2003. http://webbook.nist.gov.

Table 4. Calculated Reaction Enthalpies and Free Energies (kJ/mol)[a,b] for Reactions Involving $S_2I_4^{2+}$ [c,d]

	reactions	ΔH A	ΔH B	ΔH C	ΔH D	ΔG A	ΔG B	ΔG C
1	$S_2I_4^{2+}(g) + I_2(g) \rightarrow 2SI_3^+(g)$	−206	−244	−272	−285	−210	−246	−274
	$S_2I_4^{2+}(SO_2) + I_2(SO_2) \rightarrow 2SI_3^+(SO_2)$	75	30	5		77	31	6
	$S_2I_4^{2+}(HSO_3F) + I_2(HSO_3F) \rightarrow 2SI_3^+(HSO_3F)$	94	49	24		96	50	25
	$S_2I_4(AsF_6)_2(s) + I_2(s) \rightarrow 2SI_3(AsF_6)(s)$	366	328	300	287			
2	$S_2I_4^{2+}(g) \rightarrow 2SI_2^+(g)$	−179	−223	−241	−220	−224	−266	−284
	$S_2I_4^{2+}(SO_2) \rightarrow 2SI_2^+(SO_2)$	66	14	1		71	17	4
	$S_2I_4^{2+}(HSO_3F) \rightarrow 2SI_2^+(HSO_3F)$	82	30	17		88	35	22
	$S_2I_4(AsF_6)_2(s) \rightarrow 2SI_2(AsF_6)(s)$	265	221	203	224			
3	$S_2I_4^{2+}(g) \rightarrow S_2I^+(g) + I_3^+(g)$	−161	−191	−190	−202	−205	−233	−232
	$S_2I_4^{2+}(SO_2) \rightarrow S_2I + (SO_2) + I_3^+(SO_2)$	68	33	37		73	37	41
	$S_2I_4^{2+}(HSO_3F) \rightarrow S_2I + (HSO_3F) + I_3^+(HSO_3F)$	83	47	52		90	53	57
	$S_2I_4(AsF_6)_2(s) \rightarrow S_2I(AsF_6)(s) + I_3(AsF_6)(s)$	289	259	260	248			
4	$S_2I_4^{2+}(g) \rightarrow S_2I^+(g) + {}^2/_3I_2^+(g) + {}^1/_3I_5^+(g)$	−149	−183	−175	−206	−190	−221	−213
	$S_2I_4^{2+}(SO_2) \rightarrow S_2I^+(SO_2) + {}^2/_3I_2^+(SO_2) + {}^1/_3I_5^+(SO_2)$	79	39	51		85	44	55
	$S_2I_4^{2+}(HSO_3F) \rightarrow S_2I^+(HSO_3F) + {}^2/_3I_2^+(HSO_3F) + {}^1/_3I_5^+(HSO_3F)$	94	54	65		101	60	71
	$S_2I_4(AsF_6)_2(s) \rightarrow S_2I(AsF_6)(s) + {}^2/_3I_2(AsF_6)(s) + {}^1/_3I_5(AsF_6)(s)$	288	254	262	231			
5	$S_2I_4^{2+}(g) \rightarrow S_2I^+(g) + {}^1/_3I_4^{2+}(g) + {}^1/_3I_5^+(g)$	−66	−93	−89	−102	−94	−119	−115
	$S_2I_4^{2+}(SO_2) \rightarrow S_2I^+(SO_2) + {}^1/_3I_4^{2+}(SO_2) + {}^1/_3I_5^+(SO_2)$	71	41	47		75	44	50
	$S_2I_4^{2+}(HSO_3F) \rightarrow S_2I^+(HSO_3F) + {}^1/_3I_4^{2+}(HSO_3F) + {}^1/_3I_5^+(HSO_3F)$	80	50	56		85	54	60
	$S_2I_4(AsF_6)_2(s) \rightarrow S_2I(AsF_6)(s) + {}^1/_3I_4(AsF_6)_2(s) + {}^1/_3I_5(AsF_6)(s)$	216	189	193	180			
6	$S_2I_4^{2+}(g) \rightarrow S_2^+(g) + {}^1/_2I_3^+(g) + {}^1/_2I_5^+(g)$	−128	−162	−213	−166	−166	−199	−249
	$S_2I_4^{2+}(SO_2) \rightarrow S_2^+(SO_2) + {}^1/_2I_3^+(SO_2) + {}^1/_2I_5^+(SO_2)$	79	43	-4		86	48	2
	$S_2I_4^{2+}(HSO_3F) \rightarrow S_2^+(HSO_3F) + {}^1/_2I_3^+(HSO_3F) + {}^1/_2I_5^+(HSO_3F)$	93	56	10		101	64	17
	$S_2I_4(AsF_6)_2(s) \rightarrow S_2(AsF_6)(s) + {}^1/_2I_3(AsF_6)(s) + {}^1/_2I_5(AsF_6)(s)$	254	200	169	216			
7	$S_2I_4^{2+}(g) \rightarrow {}^1/_2S_4^{2+}(g) + {}^1/_2I_3^+(g) + {}^1/_2I_5^+(g)$	46	−6	−85	−24	32	−19	−98
	$S_2I_4^{2+}(SO_2) \rightarrow {}^1/_2S_4^{2+}(SO_2) + {}^1/_2I_3^+(SO_2) + {}^1/_2I_5^+(SO_2)$	70	18	−54		71	18	−53
	$S_2I_4^{2+}(HSO_3F) \rightarrow {}^1/_2S_4^{2+}(HSO_3F) + {}^1/_2I_3^+(HSO_3F) + {}^1/_2I_5(HSO_3F)$	70	19	−52		73	21	−50
	$S_2I_4(AsF_6)_2(s) \rightarrow {}^1/_2S_4(AsF_6)_2(s) + {}^1/_2I_3(AsF_6)(s) + {}^1/_2I_5(AsF_6)(s)$	236	184	105	166			
8	$S_2I_4^{2+}(g) \rightarrow S_2^+(g) + {}^1/_3I_2^+(g) + {}^2/_3I_5^+(g)$	−122	−158	−205	−168	−158	−193	−240
	$S_2I_4^{2+}(SO_2) \rightarrow S_2^+(SO_2) + {}^1/_3I_2^+(SO_2) + {}^2/_3I_5^+(SO_2)$	85	46	3		91	52	9
	$S_2I_4^{2+}(HSO_3F) \rightarrow S_2^+(HSO_3F) + {}^1/_3I_2^+(HSO_3F) + {}^2/_3I_5^+(HSO_3F)$	98	60	17		106	67	24
	$S_2I_4(AsF_6)_2(s) \rightarrow S_2(AsF_6)(s) + {}^1/_3I_2(AsF_6)(s) + {}^2/_3I_5(AsF_6)(s)$	253	217	170	207			
9	$S_2I_4^{2+}(g) \rightarrow {}^1/_2S_4^{2+}(g) + {}^1/_3I_2^+(g) + {}^2/_3I_5^+(g)$	52	−2	−78	−26	40	−13	−89
	$S_2I_4^{2+}(SO_2) \rightarrow {}^1/_2S_4^{2+}(SO_2) + {}^1/_3I_2^+(SO_2) + {}^2/_3I_5^+(SO_2)$	75	21	−47		77	22	−46
	$S_2I_4^{2+}(HSO_3F) \rightarrow {}^1/_2S_4^{2+}(HSO_3F) + {}^1/_3I_2^+(HSO_3F) + {}^2/_3I_5^+(HSO_3F)$	76	22	−46		79	24	−43
	$S_2I_4(AsF_6)_2(s) \rightarrow {}^1/_2S_4(AsF_6)_2(s) + {}^1/_3I_2(AsF_6)(s) + {}^2/_3I_5(AsF_6)(s)$	233	179	103	155			
10	$S_2I_4^{2+}(g) \rightarrow S_2I_2^+(g) + I_2^+(g)$	−165	−201	−204	−230	−206	−239	−242
	$S_2I_4^{2+}(SO_2) \rightarrow S_2I_2^+(SO_2) + I_2^+(SO_2)$	66	24	25		69	27	28
	$S_2I_4^{2+}(HSO_3F) \rightarrow S_2I_2^+(HSO_3F) + I_2^+(HSO_3F)$	82	39	40		86	43	44
	$S_2I_4(AsF_6)_2(s) \rightarrow S_2I_2(AsF_6)(s) + I_2(AsF_6)(s)$	255	219	216	190			

[a] Methods and basis sets: A = MPW1PW91/3-21G*, B = MPW1PW91/6-311+G(d), C = MPW1PW91/6-311+G(3df)//MPW1PW91/6-311+G(d), D = CCSD(T)/SDB-cc-pVTZ//CCSD/SDB-cc-pVTZ. [b] The reaction enthalpies and free energies were corrected to 298.15 K. [c] The dissociation energy for S_4^{2+} to $2S_2^+$ is calculated at different levels to be −348 (A), −312 (B), −254 (C), and −284 (D) kJ/mol, and the dissociation energy for I_4^{2+} to give $2I_2^+$ is calculated to be −250 (A), −270 (B), −258 (C), and −316 (D) kJ/mol (see ref 28). [d] Calculated geometries of all species are included in the Supporting Information, sections 9 and 10.

constants for bonds involving heavier elements (e.g., the Ga−Ga multiple bonds in $Ga_2H_6^{2-}$, $Ga_2H_4^{2-}$, and $Ga_2H_2^{2-}$; see the Introduction)[39] show only a slightly increasing force constant for the "double" and "triple" bonds. Comparison of our data with force constants of other heavier main group, multiple-bonded species is difficult because of a lack of experimental data. A normal-coordinate analysis of the Si═Si double bond showed that the Si═Si stretching vibration is highly coupled,[41] but calculations of the Si−Si bond strength showed only a slight increase going from the single to the triple bond.[42] In the P═P case, the force constant of the double bond (3.2 mdyn/Å) is less than twice the force constant of the single bond (1.9 mdyn/Å).[41a] In contrast, the force constant in $S_2I_4^{2+}$ (5.08 mdyn/Å) is slightly greater than double that of the S−S single bond in HSSH (2.5 mdyn/Å),[43] which is in agreement with the greater π bond strength for the S−S bond.[44]

3.3. Stability of $S_2I_4^{2+}$ and SI_3^+ in All Phases. In the gas phase, theoretical calculations show that $S_2I_4^{2+}$ is thermodynamically unstable with respect to a large range of possible dissociation products, especially to monocations (see Table 4). The reaction of $S_2I_4^{2+}(g)$ with $I_2(g)$ to give $2SI_3^+(g)$ is favored by 206−285 kJ/mol, depending on the method and basis set used. Because the energies are strongly level and basis set dependent for all energies discussed below, a range (MPW1PW91/3-21G* to CCSD(T)/SDB-cc-pVTZ) is given (see Table 4). Since the publication of our previous paper on $S_2I_4(MF_6)_2$,[10b] a reliable means to determine lattice enthalpies from the molecular volumes has been derived.[45]

(41) (a) Garbuzova, I. A.; Leites, L. A.; Bukalov, S. S. *J. Mol. Struct.* **1997**, *410*−*411*, 467−470. (b) Leites, L. A.; Bukalov, S. S.; Garbuzova, I. A.; West, R.; Mangette, J.; Spitzner, H. *J. Organomet. Chem.* **1997**, *536*−*537*, 425−432.

(42) Grunenberg, J. *Angew. Chem.* **2001**, *113*, 4150−4153; *Angew. Chem., Int. Ed.* **2001**, *40*, 4027−4029.

(43) Winnewisser, B. P.; Winnewisser, M. *Z. Naturforsch., A: Phys. Sci.* **1968**, *23A*, 832−839.

(44) Galbraith, J. M.; Blank, E.; Shaik, S.; Hiberty, P. C. *Chem.*−*Eur. J.* **2000**, *6*, 2425−2434.

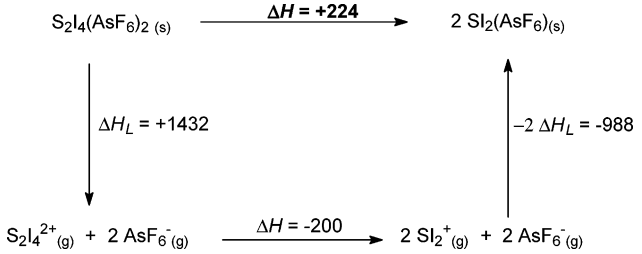

Figure 7. Born−Fajans−Haber cycle for the dissociation of $S_2I_4(AsF_6)_2$-(s) to $2SI_2(AsF_6)$(s). The energies are given in kJ/mol and are based on the CCSD(T)/SDB-cc-pVTZ//CCSD/SDB-cc-pVTZ calculations.

This equation has been successfully applied in estimating the energetics of the homopolyatomic cations of groups 16 and 17[7] and related salts in the solid state.[24a,46] If the X-ray structure of the salts is known, as is the case for $S_2I_4(MF_6)_2$-(s), then the lattice enthalpy is derived from eq 3, where α and β are coefficients of best fit, z_+ and z_- are the respective charges, ν is the number of ions per molecule, and V (nm^3) is the molecular volume [α = 117.3 kJ·nm/mol and β = 51.9 kJ/mol (1:1 salt); α = 133.5 kJ·nm/mol and β = 60.9 kJ/mol (1:2 salt)].[45] Because the lattice enthalpy is proportional to $V^{-1/3}$, any error in volume estimation leads to very small errors in the lattice enthalpy.

$$U_{POT} = |z_+||z_-|\nu\left(\frac{\alpha}{\sqrt[3]{V}} + \beta\right) \quad (3)$$

The values of the enthalpies of the dissociation reactions of $S_2I_4^{2+}$ in all phases are included in Table 4. In the solid state, $S_2I_4^{2+}$ is isolated as the $S_2I_4(MF_6)_2$ salts, even though it is unstable in the gas phase. This is because the lattice energy of the 2:1 salt is greater than that of twice the 1:1 salt, offsetting the favorable gas-phase dissociation energy. Thus, the dissociation of $S_2I_4(AsF_6)_2$(s) to $2SI_2(AsF_6)$(s) shown in Figure 7, where the lattice energy of $S_2I_4(AsF_6)_2$ is 444 kJ/mol greater than twice that of $SI_2(AsF_6)$, more than offsets the energy of dissociation of $S_2I_4^{2+}$(g) to $2SI_2^+$(g) (ΔH = −179 to −241 kJ/mol, depending on the methods and basis sets used). The situation is similar for dissociation reactions to various other products. In all cases, $S_2I_4(AsF_6)_2$(s) is shown to be stable.

The solid $S_2I_4(AsF_6)_2$ is also stable toward the addition of I_2 to give $2SI_3(AsF_6)$(s) by 287−366 kJ/mol, as shown in Figure 8. Our previous estimate gave a value of 355 kJ/mol.[10b] The lattice energy of $S_2I_4(AsF_6)_2$ (ΔH_L = 1432 kJ/mol) and the sublimation energy of I_2 (ΔH_{sub} = 62.4 kJ/mol)[47] are 570 kJ/mol greater than the favorable (ΔH = −206 to −285 kJ/mol) gas-phase reaction of $S_2I_4^{2+}$ and I_2 to give $2SI_3^+$. Thus, attempts[10] to prepare $SI_3(AsF_6)$(s) containing the classical σ-bonded SI_3^+ (isoelectronic to PI_3) lead only to the isolation of $S_2I_4(AsF_6)_2$(s) and I_2(s).

In contrast to the situation in the gas and solid phases, the enthalpies and free energies of the equilibria of $S_2I_4^{2+}$ and

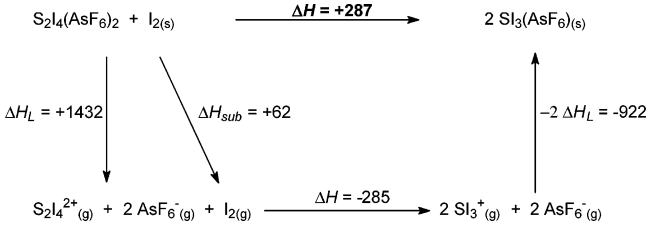

Figure 8. Born−Fajans−Haber cycle for the formation of $SI_3(AsF_6)$. The energies are given in kJ/mol and are based on the CCSD(T)/SDB-cc-pVTZ//CCSD/SDB-cc-pVTZ calculations.

its dissociation products in SO_2 and HSO_3F are small and depend on the method of calculation employed. In general, they are positive; however, equilibria involving the formation of S_4^{2+} as shown in eqs 4 and 5 are borderline or favored.

$$S_2I_4^{2+}(solv) \rightarrow {}^1/_2S_4^{2+}(solv) + {}^1/_2I_3^+(solv) + {}^1/_2I_5^+(solv) \quad (4)$$

$$S_2I_4^{2+}(solv) \rightarrow {}^1/_2S_4^{2+}(solv) + {}^1/_3I_2^+(solv) + {}^2/_3I_5^+(solv) \quad (5)$$

To obtain some experimental evidence for the species in solution, $S_2I_4(AsF_6)_2$ was dissolved in SO_2, AsF_3, and HSO_3F as a pure compound or with an excess of AsF_5 or I_2 and the solution was studied by FT-Raman spectroscopy (selected spectra are included in the Supporting Information). Unfortunately, the quality of the solution spectra was rather low. Nevertheless, some conclusions can be drawn. In SO_2 (ϵ = 12)[48] and AsF_3 (ϵ = 35),[48] the peaks due to $S_2I_4^{2+}$ either are not observed or have very low intensities; instead, peaks due to iodine cations appear, suggesting a dissociation of $S_2I_4^{2+}$ in solvents with low dielectric constants. Thus, dissociation into sulfur cations (S_4^{2+}), iodine cations (I_2^+, I_3^+, and I_5^+), or sulfur−iodine cations (SI_2^+, S_2I^+, and $S_2I_2^+$) has to be taken into account. Only in HSO_3F, a solvent with a high dielectric constant (ϵ = 120),[48] and in an excess of AsF_5, which gives a solution of the superacid HSO_3F·AsF_5, is the major species in solution determined to be $S_2I_4^{2+}$ (peaks at 735 w, 227 m, 202 m, and 163 s cm^{-1}; see Figures 7 and 8 in the Supporting Information); in addition, under these conditions, no iodine cations are observed. The spectra in SO_2 and AsF_3 show peaks in the S−S region at lower wavenumbers (e.g., 715 cm^{-1}) than they do for $S_2I_4^{2+}$, giving some evidence for the presence of S−S-bond-containing species (e.g., S_2I^+ and $S_2I_2^+$). The spectra containing an excess of iodine do not show peaks that could be assigned to SI_3^+; instead, iodine cations are observed, indicating that SI_3^+ is not formed in solution.

The calculations show that $S_2I_4^{2+}$ is least likely to dissociate in HSO_3F (ϵ = 120),[48] with high concentrations further inhibiting dissociation. This corresponds to our experimental findings. $S_2I_4^{2+}$ was observed by FT-Raman spectroscopy in solutions of HSO_3F/AsF_5 (ϵ > 130), in which $S_2I_4(AsF_6)_2$ has high solubility. In addition, the calculations show that the reaction of $S_2I_4(AsF_6)_2$ with I_2 to give $2SI_3$-(AsF_6) in all solvents is unfavorable by all methods

(45) Jenkins, H. D. B.; Roobottom, H. K.; Passmore, J.; Glasser, L. *Inorg. Chem.* **1999**, *38*, 3609−3620.
(46) Cameron, T. S.; Dionne, I.; Jenkins, H. D. B.; Parsons, S.; Passmore, J.; Roobottom, H. K. *Inorg. Chem.* **2000**, *39*, 2042−2052.
(47) *Thermodynamic Properties of Individual Substances*, 4th ed.; Gurvich, L. V., Veyts, I. V., Alcock, C. B., Eds.; Hemisphere Publishing Co.: New York, 1989.
(48) *CRC Handbook of Chemistry and Physics*, 75th ed.; Lide, D. R., Ed.; CRC Press: Boca Raton, FL, 1994.

Table 5. Summary of $S_2I_4^{2+}$ Bond Orders Determined by Different Methods

	Pauling AsF_6^-	Pauling AsF_6^- [10]	Pauling SbF_6^- [10]	$X-Y$ stretching frequency	normal-coordinate analysis
S−S	2.4	2.4	2.7	2.2	2.2
I−I	1.3	1.3	1.4	1.3	1.3
S−I	0.15/0.03	0.1/0.0	0.1		

employed, and consistently, the FT-Raman spectra of all solutions of $S_2I_4(AsF_6)_2/I_2$ showed no evidence for the formation of SI_3^+. The solutions of $S_2I_4(AsF_6)_2$ with excess I_2 in SO_2, with an empirical formula $SI_{4.5}(AsF_6)$, that were previously reported[10] most probably contain homopolyatomic cations of iodine as well as sulfur−iodine cations.

4. Conclusions

4.1. Experimental Evidence for the S−S Bond Order of 2.2−2.4 in $S_2I_4^{2+}$. In this paper, we present experimental evidence confirming that the S−S bond in $S_2I_4^{2+}$ has a bond order of 2.2−2.4. This is of the same range as the bond orders calculated for the Si−Si bonds in *trans*-RSiSiR [R = H, Me, Ph] of 1.9−2.4,[3b,3c] although it is lower than the calculated Wiberg bond index for the Si−Si bond in $[(Me_3Si)_2CH]_2(^iPr)SiSiSiSi(^iPr)[CH(SiMe_3)_2]_2$ of 2.618.[5e]

It has yet to be determined whether the S−S bond in $S_2I_4^{2+}$ or the Si−Si bond in $[(Me_3Si)_2CH]_2(^iPr)SiSiSiSi(^iPr)[CH(SiMe_3)_2]_2$ has the highest bond order, and it is reasonable to propose that they are in the same range and that they are the highest bond orders between heavier main-group elements. We note that the multiple bonds in $S_2I_4^{2+}$ are not sterically protected and that $S_2I_4^{2+}$ in the solid state maximizes π bond formation.

The X-ray structure of $S_2I_4(AsF_6)_2$ was redetermined at low temperature, FT-Raman and IR spectra were obtained, and a normal-coordinate analysis was carried out. The structure determination at low temperature allowed the correct modeling of the partly disordered AsF_6^- anions and gave a more exact distance for the crucial S−S bond [1.842(4) Å], indicating a bond order of 2.4. The geometry was modeled by theoretical methods for the first time, and the assignments of the vibrational spectra were aided by the calculated vibrational frequencies and intensities. FT-Raman and IR spectra of both salts were measured for the first time. The stretching frequency of the S−S bond was 734 cm^{-1} and indicates a bond order of 2.2. Normal-coordinate analysis yielded force constants for the S−S (5.08 mdyn/Å) and I−I bonds (1.95 mdyn/Å) and corresponding bond orders of 2.2 and 1.3, respectively. Bond orders between 2.2 and 2.4 for the S−S bond and between 1.3 and 1.4 for the I−I bond were established independent of the physical method employed (Table 5). A theoretical analysis of the bonding in $S_2I_4^{2+}$ also gives corresponding high S−S and I−I bond orders. These findings as well as AIM, NBO, and ELF analyses and a study of higher-energy isomers of $S_2I_4^{2+}$ will be the subject of another publication.

SSF_2 is also highly multiply bonded and has an S−S stretching frequency (761 cm^{-1})[49] that is greater than that for $S_2I_4^{2+}$ (734 cm^{-1}). The force constant (5.10 mdyn/Å) is only marginally higher than that for $S_2I_4^{2+}$ (5.08 mdyn/Å). The S−S stretching frequencies for both salts of $S_2I_4^{2+}$ are essentially equal, implying that the S−S distances are also equal. Given the standard deviations in the S−S distances in both salts of $S_2I_4^{2+}$ and that they are both equal, the S−S distance in $S_2I_4^{2+}$ is definitely less than that observed in SSF_2(g). Thus, we conclude that the S−S bond order in $S_2I_4^{2+}$ is greater than that in SSF_2. We hope that the multiple bonding in $S_2I_4^{2+}$ and other multiply bonded species in groups 16 and 17 will be included in the ongoing controversial but fruitful discussions on multiple bonding between heavier main-group compounds.

4.2. Energetics and Electrostatic Keys to Understanding the Behavior of $S_2I_4^{2+}$ in All Phases. $S_2I_4^{2+}$, like many polyatomic multiply charged ions, is unstable in the gas phase towards dissociation into various monocations [e.g., $S_2I_4^{2+}(g) \rightarrow 2SI_2^+(g)$, $\Delta H = -200$ kJ/mol].[50] The addition of I_2 is also favored [$S_2I_4^{2+}(g) + I_2(g) \rightarrow 2SI_3^+(g)$, $\Delta H = -285$ kJ/mol]. In contrast, in the solid state, the reactions are reversed [$S_2I_4(AsF_6)_2(s) \rightarrow 2SI_2(AsF_6)(s)$, $\Delta H = +224$ kJ/mol; $S_2I_4(AsF_6)_2 + I_2(s) \rightarrow 2SI_3(AsF_6)(s)$, $\Delta H = +287$ kJ/mol]. Thus, in the gas phase, the highly multiply bonded S−S bond in $S_2I_4^{2+}$ is less stable than that in $2SI_2^+$, containing sulfur−iodine bonds that were at one time thought to be nonexistent.[51] In both cases, the greater lattice enthalpy of the 2:1 salt, relative to 2 equivs of the 1:1 salt, more than compensates for the unfavorable gas-phase terms. This situation is reminiscent of Ca^{2+} and Ca^+. In the gas phase, Ca^+, SI_2^+, and SI_3^+ are stable, but in the solid phase, Ca^{2+} (all salts) and $S_2I_4^{2+}$ (MF_6^- salts) are energetically favored. Thus, $S_2I_4^{2+}$ and its multiple bonds are *lattice stabilized* in the solid state. The geometry of $S_2I_4^{2+}$ also maximizes positive-charge delocalization, as shown in Figure 6. A σ bonded P_2I_4[52] (isoelectronic with $S_2I_4^{2+}$) structure of $S_2I_4^{2+}$ is higher in energy. This and related topics are the subject of a separate publication.

In contrast to the gas and solid phases, where the energetics are clear cut, the net calculated energy changes of the corresponding reactions in solution are smaller. In addition, the experimental FT-Raman spectra were often marginal.

(49) We note that the S−S stretching vibration in SSF_2 is highly coupled with an S−F vibration of the same symmetry, resulting in a higher S−S frequency than that for the pure vibration.
(50) (a) Boldyrev, A. I.; Gutowski, M.; Simons, J. *Acc. Chem. Res.* **1996**, *29*, 497−502. (b) Schröder, D.; Schwarz, H. *J. Phys. Chem. A* **1999**, *103*, 7385−7394. (c) Dreuw, A.; Cederbaum, L. S. *Chem. Rev.* **2002**, *102*, 181−200.
(51) (a) Dasent, W. E. *Nonexistent Compounds*; Dekker: New York, 1965. (b) Klapötke, T.; Passmore, J. *Acc. Chem. Res.* **1989**, *22*, 234−240.
(52) Leung, Y. C.; Waser, J. *J. Phys. Chem.* **1956**, *60*, 539−543.
(53) Steudel, R. *Angew. Chem.* **1975**, *87*, 683−692; *Angew. Chem., Int. Ed. Engl.* **1975**, *14*, 655−664 and references therein.
(54) Passmore, J.; Sutherland, G.; Taylor, P.; Whidden, T. K.; White, P. S. *Inorg. Chem.* **1981**, *20*, 3839−3845.
(55) Dionne, I. Ph.D. Thesis, University of New Brunswick: Fredericton, NB, Canada, 2002.
(56) Mardsen, C. J.; Oberhammer, H.; Lösking, O.; Willner, H. *J. Mol. Struct.* **1989**, *193*, 233−245.
(57) Howard, W. F., Jr.; Andrews, L. *J. Am. Chem. Soc.* **1975**, *97*, 2956−2959.
(58) Balhius, F.; Koster, P. B.; Migchelsen, T. *Acta Crystallogr.* **1967**, *23*, 90−91.
(59) Davies, C. G.; Gillespie, R. J.; Ireland, P. R.; Sowa, J. M. *Can. J. Chem.* **1974**, *52*, 2048−2052.
(60) Howard, W. F.; Andrews, L. *J. Raman Spectrosc.* **1974**, *2*, 447−462.
(61) Hesselmann, A.; Jansen, G. *Chem. Phys. Lett.* **2003**, *367*, 778−784.

However, energetics favored undissociated $S_2I_4^{2+}$ in solvents of high dielectric constants, and consistently, FT-Raman spectra showed that it is present in HSO_3F/AsF_5. Calculations showed SI_3^+ to be unstable in solution, and consistently, it was not detected by Raman spectroscopy. We previously found that addition of I_2 to $S_2I_4(MF_6)_2$ increased its solubility in SO_2 and gave solutions of the average empirical formula $SI_{4.5}AsF_6$.[10] FT-Raman spectra of these solutions showed the presence of homopolyatomic cations of iodine as well as the presence of an unknown that could be a sulfur−iodine cation.

Acknowledgment. We thank the Natural Sciences and Engineering Research Council (NSERC) of Canada for funding (J.P.) and a Graduate Scholarship (S.B.) and the Alexander von Humboldt Foundation in Germany for providing a Feodor-Lynen Fellowship (C.K.) and a Visiting Research Fellowship (J.P.). The Ministry of Education in Finland and the Academy of Finland are also gratefully acknowledged for providing financial support (J.M.R.).

Supporting Information Available: X-ray structural data for $S_2I_4(AsF_6)$ (CIF); cation−anion contacts in $S_2I_4(AsF_6)_2$; bond valence maps for the AsF_6^- anions; discussion of why one AsF_6^- anion is disordered; packing in the structure of $S_2I_4(AsF_6)_2$; determination of solution FT-Raman spectra; visualization of the calculated vibrational modes of $S_2I_4^{2+}$; FT-Raman spectrum of $S_2I_4(SbF_6)_2$ in HSO_3F/AsF_5; FT-Raman spectrum of $S_2I_4(SbF_6)_2$ in SO_2; calculation of the geometry and the vibrational frequencies of $S_2I_4^{2+}$ using different methods and basis sets; estimation of S−S and I−I bond orders; estimation of the enthalpy of the reaction of $S_2I_4(SbF_6)_2$ with I_2 to give $2SI_3(AsF_6)$; estimation of molecular (ion) volumes; calculated geometries for all sulfur, iodine, and sulfur−iodine species; visualization of the calculated geometries. This material is available free of charge via the Internet at http://pubs.acs.org.

IC049035G

(62) (a) Rosenstock, H. M.; Draxl, K.; Steiner, B. W.; Herron, J. T. *J. Phys. Chem. Ref. Data* **1977**, *6* (Suppl. 1). (b) Wagman, D. D.; Evans, W. H.; Parker, V. B.; Schumm, R. H.; Halow, J.; Bailey, S. M.; Chruney, K. L.; Nuttall, R. L. *J. Phys. Chem. Ref. Data* **1982**, *11* (Suppl. 2).